IIETA International Information and Engineering Technology Association
Advancing the World of Information and Engineering

Journal Européen des Systèmes Automatisés
Vol. 58, No. 11, November, 2025, pp. 2405-2415
Journal homepage: http://iieta.org/journals/jesa

Barrier Function Based Integral Sliding Mode Control for Attitude Control of Rigid Spacecraft

Osamah A. Aldoori[1*], Mohammed Y. Hassan[2], Abbas H. Issa[3]

[1] College of Control and Systems Engineering, University of Technology, Baghdad 10066, Iraq
[2] College of Artificial Intelligence Engineering, University of Technology, Baghdad 10066, Iraq
[3] College of Electrical Engineering, University of Technology, Baghdad 10066, Iraq

Corresponding Author Email: cse.22.02@grad.uotechnology.edu.iq

https://doi.org/10.18280/jesa.581117

Received: 5 October 2025
Revised: 3 November 2025
Accepted: 12 November 2025
Available online: 30 November 2025

Keywords:
BF, SMC, Adaptive SMC, ISMC, rigid spacecraft model, BFASMC

ABSTRACT

This study introduces a recent robust control method for attitude control of a rigid spacecraft using barrier function (BF) based integral sliding mode control (BFISMC). BFISMC scheme combines all the features of the classical integral sliding mode control (ISMC) with the continuity characteristic of BF to provide two major features, the first, the perturbation ultimate bound or its derivative is not needed to be known in advance, and secondly, eliminate the chattering phenomenon related to Conventional Sliding Mode Control (CSMC) and ISMC. The proposed method mechanism aims to ensure the system states in predefined vicinity to zero from the first instant. Comparison was performed with the conventional integral sliding mode control (CISMC) and adaptive sliding mode control based on BF (BFASMC) to demonstrate the strength of the proposed method against them. The results showed improved adaptability, robustness, smoother control input (CI) and minimum control effort. The effectiveness of the proposed approach is validated by simulation results of satellite attitude control with certain Moment of Inertia (MOI) and assumed external severe time varying disturbances. As the results, show the proposed controller tracks the states to desired trajectories accurately with steady sate error up to (2.8×10^{-3} rad) and minimize control effort down to (0.33 nm) with excellent adaptation, disturbance reduction and chattering elimination. The stability of ISMC and BFISMC are confirmed by Lyapunov criteria.

1. INTRODUCTION

Spacecrafts often experience difficult conditions in space, represented by several forces that threaten their attitude and even their stability, such as gravitational force, aerodynamic drag, solar pressure, and others. In addition to this, there are the complexities of the nonlinear dynamics and Moment of Inertia (MOI) uncertainty. Given the importance of spacecraft, which have come to play a dominant role in several fields, such as communications, weather forecasting, monitoring, and guidance, the need to develop control over their positioning and stability has become indispensable.

Over the past decades, several methods have been developed to deal with these problems. These methods include the adaptive control [1-3], Sliding mode control [4-6], back-stepping control [7, 8], and fuzzy control [9, 10]. Through these approaches, the sliding mode control is one of the most effective strategies for attitude control of rigid spacecraft.

The use of Sliding Mode Control (SMC) for attitude controlling of rigid spacecraft was originally introduced in the study [11], after which several types of SMC control were introduced by researchers such as Conventional CSMC where convergence is asymptotic [12-15]. Unlike CSMC, Terminal SMC (TSMC) was used to ensure convergence at a specific time [16-18]. Then a modified TSMC was used to avoid singularity while ensuring convergence in finite time called Fast (FTSMC) [19-22]. However, in both cases, despite ensuring the speed of convergence and avoiding the singularity, global robustness cannot be guaranteed due to the presence of the reaching phase. To eliminate this situation, ISMC was resorted to, which is characterized by no reaching phase. Therefore, TISMC was introduced to ensure global robustness and convergence in a finite time [23, 24]. A fixed-time ISMC was introduced in the study [25] to eliminate the reaching phase operations and ensure convergence in a fixed time with global robustness.

However, all of the above studies rely on prior knowledge of the upper bound of the disturbance and uncertainties.

In the case where the upper bound of disturbance is unknown there are two main different ways for adaptive Sliding Mode Control (ASMC) [26]. The first method involves increasing the gain until the sliding mode (SM) is reached, after which the gain value stays stationary to ensure the ideal SM for a while. However, SM can be lost when disturbance increases and the gain value will increase to reattain the SM [27, 28]. Second method presented by the study [29] is based on the reference model and equivalent control to estimate the disturbances. A low pass filter was used for implementation,

however, the choosing the filter gain which must be considerably lower than the inverse of the highest value of the first derivative of the disturbance is so difficult. So, many strategies are suggested by researchers, the core of these strategies is the adaptation of the controller gain as in studies [30-34] where the ASMC is proposed for attitude tracking, while a FTSMC is proposed in the study [35] to ensure finite time convergence. ASM Fault tolerant control [36] is developed as a controller for nonlinear systems, in this approach even with adaptation algorithm the dynamics of perturbation may require. While in the study [37] dynamic sliding variable and adaptation law are used to design adaptive dynamic SMC. In the study [38] Finite time attitude tracking by designing passivity _ ASMC is proposed, in this method the full state feedback is assumed, where it is practically unavailable. In addition, disturbance observer can be used to reject the disturbance and combined with ASMC for UAV trajectory tracking as in the study [39], this approach depends on parameters tuning which makes the computational process large. Moreover, fuzzy logic and neural network (NN) also played a role in attitude control, where Tkagi-Sogeno Fuzzy Algorithm combined with ASMC for spacecraft attitude controlling, the limitations of this strategy are the high computational process, chattering issue, and the precise selection of the membership function of fuzzy model [40, 41], and an adaptive fuzzy – Neural PID-Like Controller for Nonlinear MIMO Systems is presented in the study [42].

Most of Previously mentioned studies involve complex computational, in addition to reducing, rather than eliminating, the chattering. This has encouraged researchers to develop effective and simple strategies to cope with these problems, while ensuring robustness without knowing the details of the perturbationdynamics .

However, CSMC and adaptive SMC are the most effective method for controlling nonlinear systems, especially those suffering from disturbances and uncertainty, but through the reaching phase, the robust stability and performance may not be ensured. The ISMC is a special type of SMC, which is unique in that there is no reaching phase, which means the SM will be achieved from the beginning, meaning that the control system will be in nominal and full order from the first moment. However, like CSMC, it also suffers from chattering [43-46].

To cope these problems, BF based ISMC (BFISMC) has been proposed. In addition to exploiting characteristics of ISMC, the features of the presented method are:

1- The knowledge of the ultimate limit of perturbation and model uncertainties or their derivative are not required in advance.

2- There is only one control parameter to be tuned to improve the steady state error.

3- Chattering elimination because BF is continuous.

The structure of this study is organized as follows: Section 2 explains the mathematical model of a rigid spacecraft, Section 3 provides the details of ISMC, BF with ASMC (BFASMC) and the proposed BFISMC. The results and comparison will be presented in Section 4, while the conclusions will be in the Section 5.

2. RIGID SPACECRAFT MATHEMATICAL MODEL

In this paper a Satellite motion is described by the rotation about principal axis of rigid body, but first, there are some key assumptions about rigid spacecraft:

- No part of the spacecraft can be affected or deformed by any external force or disturbance.
- The flexibility of the structure, fuel flow, and vibrations are neglected.
- The total mass does not change over time, nor does its distribution.
- The MOI is constant.

Then the equation of motion will be extracted by Euler's equations [47-49].

$$T=dL/dt \tag{1}$$

$$L=I\omega \tag{2}$$

where:

T = Net external torque vector (3×3)in (n.m.)

L = Angular momentum vector (3×3) in $((kg.m^2/s)$

I = Satellite MOI matrix (3×3) in $(kg.m^2)$

ω = Angular velocity vector (3×1) in (rad/s)

In this paper a body-fixed frame (rotating with satellite) is used to avoid the complexities of the variation of I with direction in an inertial frame.

For a body – fixed frame Eq. (1) becomes:

$$\left.\frac{dL}{dt}\right|_{inertial} = \left.\frac{dL}{dt}\right|_{body} + \omega \times L \tag{3}$$

So, the rotational equation becomes:

$$T=I\dot{\omega}+ \omega \times L \tag{4}$$

$$T=I\dot{\omega}+ \omega \times (I\omega)$$

$$T_i= u_i+ d_i \ (i=1,2,3) \tag{5}$$

where, T is the applied torque, u is the control input, d is an external disturbance, and X is cross product. For principal axis & diagonal certain MOI:

$$I=\begin{bmatrix} J_1 & 0 & 0 \\ 0 & J_2 & 0 \\ 0 & 0 & J_3 \end{bmatrix}, \omega=\begin{bmatrix} \omega_1 \\ \omega_2 \\ \omega_3 \end{bmatrix}, \dot{\omega}=\begin{bmatrix} \dot{\omega}_1 \\ \dot{\omega}_2 \\ \dot{\omega}_3 \end{bmatrix}$$

the expanding Euler's equations become:

$$\left.\begin{aligned} T_1 &= J_1\,\dot{\omega}_1 + (J_3 - J_2)\omega_2\,\omega_3 \\ T_2 &= J_2\,\dot{\omega}_2 + (J_1 - J_3)\omega_1\,\omega_3 \\ T_3 &= J_3\,\dot{\omega}_3 + (J_2 - J_1)\omega_1\,\omega_2 \end{aligned}\right\} \tag{6}$$

And

$$\left.\begin{aligned} \dot{\omega}_1 &= \frac{1}{J_1}\,[\,(J_2 - J_3)\omega_2\,\omega_3 + T_1\,] \\ \dot{\omega}_2 &= \frac{1}{J_2}\,[\,(J_3 - J_1)\omega_1\,\omega_3 + T_2\,] \\ \dot{\omega}_3 &= \frac{1}{J_3}\,[\,(J_1 - J_2)\omega_1\,\omega_2 + T_3\,] \end{aligned}\right\} \tag{7}$$

Euler's angles $(\varphi, \theta, \emptyset)$ are often describe the satellite orientation where, Roll Angle $(\emptyset)$ is the rotation around x-axis, Pitch Angle (θ) is the rotation around y-axis and Yaw Angle (φ) is the rotation around z-axis.

The body _ frame angular velocities ($\omega_1, \omega_2, \omega_3$) related to Euler angle are:

$$\begin{bmatrix}\omega_1\\ \omega_2\\ \omega_3\end{bmatrix} = \begin{bmatrix}1 & 0 & -\sin\theta\\ 0 & \cos\emptyset & \sin\emptyset\cos\theta\\ 0 & -\sin\emptyset & \cos\emptyset\cos\theta\end{bmatrix}\begin{bmatrix}\dot{\emptyset}\\ \dot{\theta}\\ \dot{\varphi}\end{bmatrix}$$

For small angles (simplified dynamics):

$$\omega_1 \approx \dot{\emptyset}, \qquad \omega_2 \approx \dot{\theta}, \qquad \omega_3 \approx \dot{\varphi} \tag{8}$$

by substituting Eqs. (5) and (8) in Eq.(7)

$$\ddot{\emptyset} = \frac{1}{J_1}[(J_2 - J_3)\dot{\theta}\dot{\varphi} + T_1] \tag{9}$$

$$\ddot{\theta} = \frac{1}{J_2}[(J_3 - J_1)\dot{\varphi}\dot{\emptyset} + T_2] \tag{10}$$

$$\ddot{\varphi} = \frac{1}{J_3}[(J_1 - J_2)\dot{\emptyset}\dot{\theta} + T_3] \tag{11}$$

Let $x_1 = \emptyset,\ x_2 = \dot{\emptyset}\ ,\ x_3 = \theta,\ x_4 = \dot{\theta},\ x_5 = \varphi,\ x_6 = \dot{\varphi}$ then:

$$\dot{x}_1 = x_2 \tag{12}$$

$$\dot{x}_2 = \frac{1}{J_1}[(J_2 - J_3)x_4x_6 + T_1] \tag{13}$$

$$\dot{x}_3 = x_4 \tag{14}$$

$$\dot{x}_4 = \frac{1}{J_2}[(J_3 - J_1)x_6x_2 + T_2] \tag{15}$$

$$\dot{x}_5 = x_6 \tag{16}$$

$$\dot{x}_6 = \frac{1}{J_3}[(J_1 - J_2)x_4x_2 + T_3] \tag{17}$$

This is a 6th order nonlinear, coupled dynamical system governing the Euler's equation of motion around principal axis.

3. CONTROLLER DESIGN

In this section ISMC and BFASMC will be introduced which are both robust controllers for the purpose of comparison and proving the superiority of the proposed controller which will be presented in the last part of this section.

3.1 Integral Sliding Mode Controller (ISMC)

CSMC consist of two phases, the reaching phase, which is the trajectory of the system from its initial state to the moment it reaches the sliding surface, at which point it enters the sliding phase, as illustrated in Figure 1. The property of robustness against disturbances or parameters variation is achieved only through the SM. Therefore, robustness cannot be guaranteed over the reaching phase [50]. The removal of the reaching phase in the CSMC is done by using the ISMC, in which the states are in the sliding phase from the first moment [51]. In ISMC the order of system dynamic in sliding mode does not change, therefore it's also called full order SMC (FOSMC), while in CSMC the order reduction of the system is due to numbers of control signals.

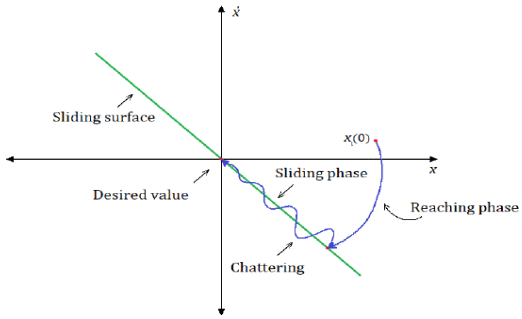

Figure 1. Sliding surface [52]

To design the ISMC, the error equations are:

$$e_1 = x_1 - x_{1d} \tag{18}$$

$$e_2 = x_3 - x_{3d} \tag{19}$$

$$e_3 = x_5 - x_{5d} \tag{20}$$

where, x_{1d}, x_{3d} and x_{5d} are the desired Roll, Pitch and Yaw rotation angles and will be chosen later as constants . The time derivative of the error equations are:

$$\dot{e}_1 = \dot{x}_1 - \dot{x}_{1d} = x_2 \tag{21}$$

$$\dot{e}_2 = \dot{x}_3 - \dot{x}_{3d} = x_4 \tag{22}$$

$$\dot{e}_3 = \dot{x}_5 - \dot{x}_{5d} = x_6 \tag{23}$$

The sliding surfaces corresponding to three control inputs are designed as:

$$s_1 = \dot{e}_1 + \rho e_1 \tag{24}$$

$$s_2 = \dot{e}_2 + \rho e_2 \tag{25}$$

$$s_3 = \dot{e}_3 + \rho e_3 \tag{26}$$

where, $\rho > 0$ is convergence rate. The time derivative of sliding surface equations are:

$$\dot{s}_1 = \dot{x}_2 + \rho x_2 \tag{27}$$

$$\dot{s}_2 = \dot{x}_4 + \rho x_4 \tag{28}$$

$$\dot{s}_3 = \dot{x}_6 + \rho x_6 \tag{29}$$

by substitution Eqs. (13), (15), and (17) in Eqs. (27-29) the following equations are obtained:

$$\dot{s}_1 = \frac{1}{J_1}[(J_2 - J_3)x_4x_6 + u_1 + d_1] + \rho x_2 \tag{30}$$

$$\dot{s}_2 = \frac{1}{J_2}[(J_3 - J_1)x_6x_2 + u_2 + d_2] + \rho x_4 \tag{31}$$

$$\dot{s}_3 = \frac{1}{J_3}[(J_1 - J_2)x_4x_2 + u_3 + d_3] + \rho x_6 \quad (32)$$

Let the control law taken as:

$$u_i = J_i(u_{ni} + u_{si})\ i = 1{,}2\ and\ 3 \quad (33)$$

u_{ni} is the nominal control to make a stabilization to system nominal dynamics, while the disturbance term will addressed by switching control law u_{si} [50].

$$u_{n1} = -\frac{1}{J_1}(J_2 - J_3)x_4x_6 - \rho x_2 - \beta_1 s_1 \quad (34)$$

$$u_{n2} = -\frac{1}{J_2}(J_3 - J_1)x_6x_2 - \rho x_4 - \beta_2 s_2 \quad (35)$$

$$u_{n3} = -\frac{1}{J_3}(J_1 - J_2)x_4x_2 - \rho x_6 - \beta_3 s_3 \quad (36)$$

$\beta_{1,2and3}$ are positive gains to be designed according to required performance. For ISMC the auxiliary sliding variable is designed as:

$$\sigma_i = s_i + z_i \quad (37)$$

s_i , z_i are conventional sliding manifold and integral term (auxiliary sliding variable) respectively such that σ_i, s_i, $z_i \in R^1$ with $z(0) = -s(0)$ which leads to $\sigma_i(0) = 0$ from the first instant.

$$\dot{\sigma}_i = u_{ni} + u_{si} + d_i + \dot{z}_i \quad (38)$$

let $\dot{z}_i = -u_{ni}$ and this leads to

$$\dot{\sigma}_i = u_{si} + d_i \quad (39)$$

by applying equivalent control to Eq. (39) yields

$$\dot{\sigma}_i|_{eq} = 0 = u_{si}|_{eq} + d_i$$
$$u_{si}|_{eq} = -d_i$$

This means, the disturbance will be eliminated by discontinuous control in equivalent mode from the first moment ($t \geq 0$).

Consequently, the equivalent close loop control systems in Eqs. (13), (15) and (17) can be given by:

$$\dot{x}_2 = \frac{1}{J_1}[(J_2 - J_3)x_4x_6 + u_{n1}] = -\beta_1 s_1 \quad (40)$$

$$\dot{x}_4 = \frac{1}{J_2}[(J_3 - J_1)x_6x_2 + u_{n2}] = -\beta_2 s_2 \quad (41)$$

$$\dot{x}_6 = \frac{1}{J_3}[(J_1 - J_2)x_4x_2 + u_{n3}] = -\beta_3 s_3 \quad (42)$$

It can be noticed that all control systems are nominal model systems with nominal control u_{ni} which can be designed to satisfy the desired performance for all ($t \geq 0$).

For the discontinuous control, it's the same of CSMC and it's given by:

$$u_{si} = -k\,sign(\sigma) \quad (43)$$

Substituting in Eq. (39)

$$\dot{\sigma}_i = -k\,sign(\sigma) + d_i \quad (44)$$

To obtain k for globally symptomatically stability, the Lyapunov candidate function:

$$V = \frac{1}{2}\sigma^2 > 0 \quad (45)$$

$$\dot{V} = \sigma\dot{\sigma} = \sigma(-k\,sign(\sigma) + d) \quad (46)$$

$$\dot{V}_i \leq -|\sigma_i|(k_i - |d_i|)$$
$$\dot{V}_i \leq 0, \text{ when } (k_i - |d_i|) > 0$$
$$|d_i| \leq d_{max}$$
$$(k_i - d_{max}) > 0$$

For negative definite, $k_i > d_{max}$.

3.2 Adaptive SMC based on Barrier Function (BFASMC)

This approach is introduced by Obeid et al. [26], in this method, and based on the magnitude of sliding manifold which is affected by disturbances and uncertainties, the increasing and decreasing of the gain is allowed. Unlike the CSMC and ISMC, the BFASMC, the knowledge of the maximum value of uncertain parameters and external disturbances is not requested in advance.

3.2.1 BF

Definition [26]: Assume that there is $\epsilon > 0$ can be selected and reformed.

BF is defined as even continuous function such as:

$B : X \in [-\epsilon, \epsilon] \rightarrow B(X) \in [N, \infty]$ and strictly increasing on $[0, \epsilon]$

$$lim_{|x| \rightarrow \epsilon} B(x) = +\infty$$

B(x) has a unique minimum at zero and B (0) =N ≥0

There are two types of BF:

1- Positive definite BF (PBF), $B_p = \frac{\epsilon N}{\epsilon - |x|}$, such as $B_p(0) = N > 0$

2- Positive semi definite BF (PSBF), $B_{ps}(x) = \frac{|x|}{\epsilon - |x|}$, such as $B_{PS}(0) = 0$

3.2.2 Adaptation algorithm

The adaptive algorithm of this method is partitioned into two stages or phases [26]. The first phase, the gain will increase to a pre-determined time t^*, at which time the gain value becomes equal to the maximum value of the disturbance to ensure a finite time convergence of sliding variable to neighbourhood of zero. Then it turns into the second phase, which is the BF.

Phase 1 (Constant gain Adaptation $t < t^*$)

Let's consider the control law as:

$$u_{si} = -k_{ci}\,sign(s)$$

and the adaptive gain law as:

$$k_{ci} = k_{ci} + \alpha|s_i| \quad (47)$$

k_{ci} is directly increasing to $|s_i|$ to ensure rapid initial adaptation, and α is the adaptation rate.

Phase 2 (BF gain $t \geq t^*$)

A positive semi-definite BF will be used in this paper

$$k_{ci} = \frac{|s_i|}{\epsilon - |s_i|} \text{PSDBF} \tag{48}$$

k_{ci} adapt to counteract disturbance and ensures s_i to stay in ($|s_i| < \epsilon$).

When s approaches zero and $\epsilon > 0$ them exist t^* which is the smallest root of inequality $|s(t)| \leq \frac{\epsilon}{2}$ such that for all $t \geq t^*$, the inequality the $|s| < \epsilon$ is satisfied [52].

3.3 The proposed BF based Integral SMC (BFISMC)

In an integral sliding controller, unlike CSMC, there is no reaching phase , but there is still a need to know the maximum value of the disturbance in advance. On the contrary, when using BFASM the advanced knowledge of the ultimate limit of the disturbance is not required, but at the same time there is a time to reach the region close to zero (reaching phase). In contrast, the proposed method, illustrated in Figure 2, provides a solution by utilizing the ISMC with the use of the BF as explained below:

From Eq. (43) the discontinuous control law for ISMC:

$$u_{si} = -\text{sign}(\sigma)$$

Using positive semi definite continuous BF as a controller gain such as:

$$u_{si} = -\frac{|\sigma_i|}{\epsilon - |\sigma_i|} \text{sign}(\sigma_i) = -k_b \frac{\sigma_i}{\epsilon - |\sigma_i|} \tag{49}$$

where, $1 \gg \epsilon > 0$ represents the boundary layer thickness and $k_b > 0$ is the gain of the controller that could be chosen for steady state error regulation and robustness improvement. The advantages of the proposed approach could be outlined as follows:

- No knowledge of the maximum value of the disturbance is to be known in advance.
- No reaching phase.
- Chattering is eliminated or (attenuated for smaller ϵ), and this is due the continuity feature of the BF within boundary layer $|s| < \epsilon$.

Calling Eqs. (45) and (46) of Lyapunov candidate function:

$$V = \frac{1}{2}\sigma^2$$

$$\dot{V} = \sigma\dot{\sigma} = \sigma(-\text{sign}(\sigma) + d)$$

$$\dot{V} = \sigma\dot{\sigma} = \sigma(-k_b \frac{\sigma_i}{\epsilon - |\sigma_i|} + d) \tag{50}$$

$$\dot{V} \leq -|\sigma| (k_b \frac{|\sigma_i|}{\epsilon - |\sigma_i|} - |d|) \tag{51}$$

For negative definiteness

$$(k_b \frac{|\sigma_i|}{\epsilon - |\sigma_i|} - |d|) > 0 \tag{52}$$

let $|d| \leq d_{max}$

$$\frac{|\sigma_i|}{\epsilon - |\sigma_i|} > d_{max} \tag{53}$$

$$k_b|\sigma_i| > (\epsilon - |\sigma_i|)\, d_{max} \tag{54}$$

$$k_b|\sigma_i| + d_{max}|\sigma_i| > d_{max}\, \epsilon \tag{55}$$

$$|\sigma_i|(k_b + d_{max}) > d_{max}\, \epsilon \tag{56}$$

$$|\sigma_i| > \frac{d_{max}\epsilon}{k_b + d_{max}} \rightarrow \dot{V} < 0 \tag{57}$$

Which means the ultimate bound of $|\sigma_i|$ is less than $\frac{d_{max}\epsilon}{k_b + d_{max}}$ which is less than ϵ, [51, 53].

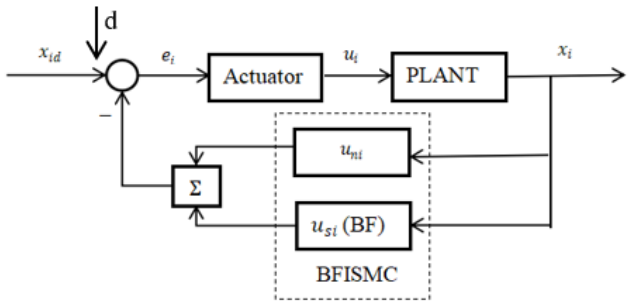

Figure 2. Block diagram of BFISMC

4. SIMULATION RESULT

The simulation will be implemented by applying three methods, ISMC, BFASMC and BFISMC, and that to demonstrate the superiority of this method over the other two methods with regard to chattering elimination and the value of the input control effort required to achieve robust stability and performance, and thatis considered the most importan element in spacecraft, which are strictly limited in energy consumption. Therefore, reaching the desired path with the .least energy consumption is an important issueMATLAB R2023a / m. file is used for simulation of the proposed controller and the other methods with variable magnitude time varying disturbances. Figure 3 represents the assumed increasing disturbance starts as time varying disturbance till time = 5 s with upper bound 0.3 and then changed to constant value of 0.7 until t = 12 s then after that the maximum absolute value will be 1.7 with same frequency, and that is to test the ability of the controller to adapt to the unexpected variation in forces affecting the system. The system parameters are introduced in Table 1 and parameters of controller are represented in Table 2.

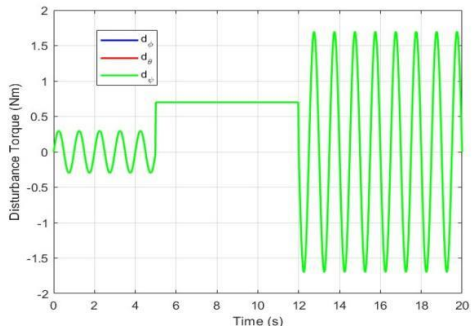

Figure 3. Applied disturbances

Table 1. Assumed system parameters

Initial Conditions ($\emptyset, \theta, \varphi$) and Their Angular Velocities	$[0; 0; 0; 0; 0; 0]^T$
Desired Values ($\emptyset, \theta, \varphi$)	$[0.8; 0; 0.5; 0; -0.8; 0]^T$
Disturbances ($d_{1,2,3}$)	$0.3sin(2\pi t) \quad 0 \le t < 5$ $0.7 \quad 5 \le t < 12$ $-1.7sin(2\pi t) \quad t \ge 12$
MOI (Diagonal certain matrix)	$J_1 = I_{XX} = 0.16$ $J_2 = I_{YY} = 0.311$ $J_3 = I_{ZZ} = 0.311$

Table 2. Controller parameters

ISMC	BFASMC	BFISMC
	$k_{init} = 0.1$	$k_{init} = 0.0$
$k_i = 2 > d_{max}$	$k_b = 0.2$	$k_b = 0.2$
$\beta_{i=6}$	$\epsilon = 0.05$	$\epsilon = 0.05$
	$t^* = 1.7s$	$t^* = 0$

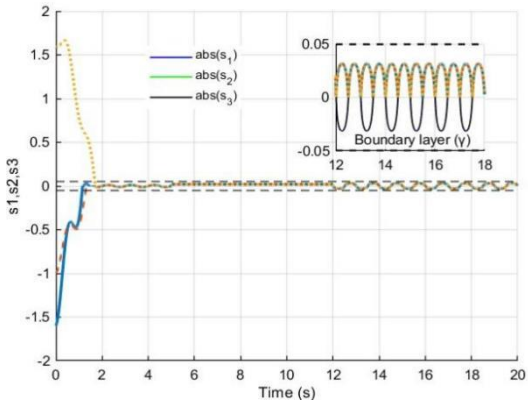

(a) BFASMC

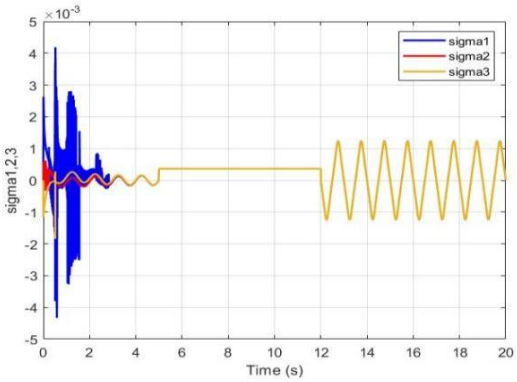

(b) ISMC sliding vvariables

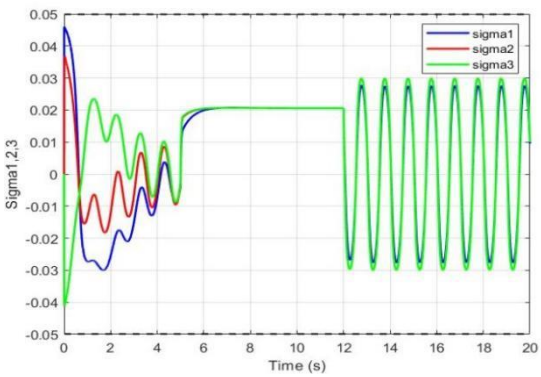

(c) BFISMC

Figure 4. Sliding variables

Figure 4 represents the convergence of the sliding variable to a region close to zero. It can be seen from Figure 4(a) that the sliding variables of BFASMC converge to a neighbourhood of zero which is defined in advance in finite time through the reaching phase, during this phase the controller gain increases due to the adaptive law to reach the upper bound of disturbances which in turn increases the control effort and may cause chattering. In Figure 4(b) and (c), it can be observed that there is no reaching phase, this is a result of using the ISMC, the sliding variable starts from the first instant. For ISMC method, the sliding variable is almost zero from the first moment, but with a small error rate which is inversely proportional to the controller gain as shown in Figure 4(a). As for Figure 4(c), which represents BFISMC methodology, it can be noted that the sliding variable is within the boundary layer from the first moment, and also that there is no chattering due to the use of the BF.

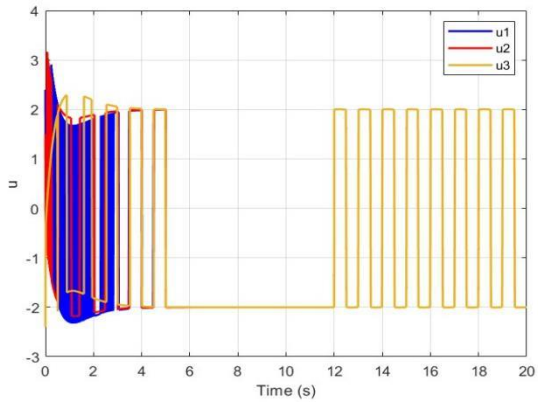

(a) ISMC

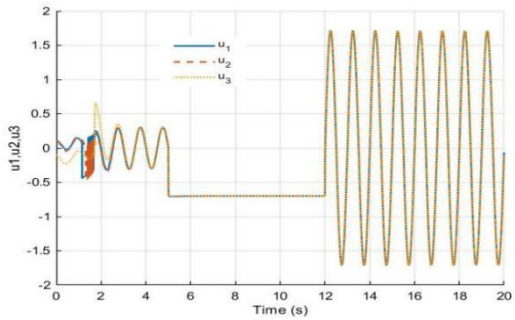

(b) BFASMC

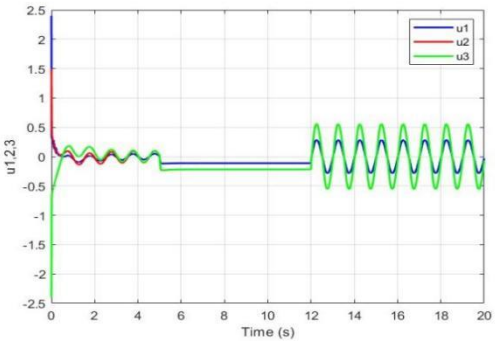

(c) BFISMC

Figure 5. Control inputs

Figure 5 represents the control input torque required applied by the reaction wheels to bring the rotation angles *(∅, θ* and *φ)* to the desired value despite the presence of disturbances. In ISMC, the value of the controller gain is constant and higher

than the maximum value of the disturbance ($k_i = 2 > |d| = 1.7$) which must be known in advance. As a result, the actuators (reaction wheels) will be exposed to the negative effect of chattering. In this simulation, the sign function was replaced by the tanh function to reduce the chattering and this is clear in Figure 5(a). While when using BFASMC method as explained in Figure 5(b) it can be seen that the control input follows the path of the disturbance completely to overcome it with no chattering except in transition from phase 1 to phase 2 (transit p1-p2) at time $t^* = 1.7s$. In contrast in Figure 5(c) the control inputs of BFISMC compensate the disturbances from the first instant with minimum continuous control effort compared to other two methods as explained in Table 3.

Table 3. Comparison between ISMC, BFASMC and BFISMC

Metrics	Angle	ISMC	BFASMC	BFISMC
Steady State Error (rad)	∅	8×10^{-6}	5.9×10^{-3}	2.6×10^{-3}
	θ	8×10^{-6}	5.9×10^{-3}	2.8×10^{-3}
	φ	8×10^{-6}	6.0×10^{-3}	2.8×10^{-3}
Root Mean Squar Error (rad)	∅	0.1492	0.1447	0.3437
	θ	0.0933	0.1005	0.2146
	φ	0.1493	0.2015	0.3439
Integral Squar Error (rad^2)	∅	0.4648	0.4187	0.4637
	θ	0.1815	0.2017	0.1807
	φ	0.4640	0.8117	0.4632
Mean Control Effort (n.m)	∅	1.99	0.7235	0.1632
	θ	1.98	0.7233	0.2773
	φ	1.97	0.7291	0.3320
Max. Control Effort (n.m.)	∅	2.9	1.711	2.4
	θ	3.16	1.721	1.5
	φ	2.4	1.711	2.4
Max. Perturbation (d_{max})		Required	Not Required	Not Required
Chattering Effect		Reduced (due to tanh function)	Transit (p1-p2)	No Chattering

Figure 6 observes the response of system states (rotation angles ∅,θ and φ) for the three methodologies with different high relative accuracy. As in Figure 6(a), the error of states response when using ISMC is very low and lower than other two methods because in ISMC the value of error is indirectly inversely proportional to the controller gain and this means that the higher the gain value, the lower the error but that will be on the account of chattering. However, when using BFASMC or BFISMC the states response error depends on the thickness of the boundary layer ($|\epsilon|$) as shown in Figures 6(b) and (c), which means that the response accuracy can be increased by decreasing this thickness, but more decreasing may cause chattering, therefore, a kind of balance between high precision and chattering must be taken into consideration.This will be more clearly illustrated in Figure 7.

Table 3 demonstrates the superiority of the proposed method over the other two methods. SSE can be observed to be reduced by more than 50% compared to BFASMC for each rotation angle, but it is larger for ISMC, with minor differences in RMSE and ISE. However, the most significant advantage of this method is the reduction in control effort by more than 70% compared to BFASMC, which is a critical issue in spacecraft design due to power consumption limitations. While in ISMC, the control effort is relatively high and constant due to the controller gain overestimation. In addition, there is no chattering in control input and no need for prior knowledge of the upper bound of the disturbances for the proposed approach, in contrast, in BFASMC a chattering exist in transition stage between phase 1 and phase 2 (transit p1-p2).

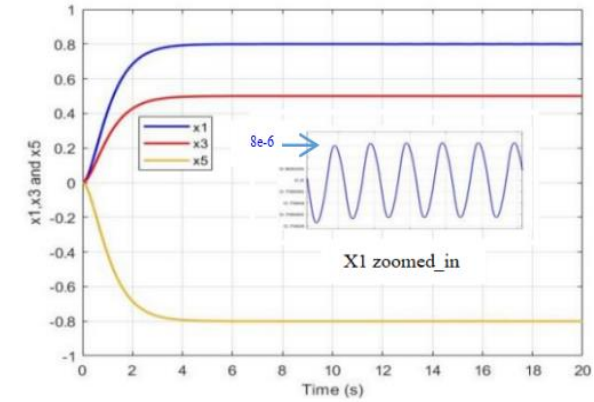

(a) ISMC

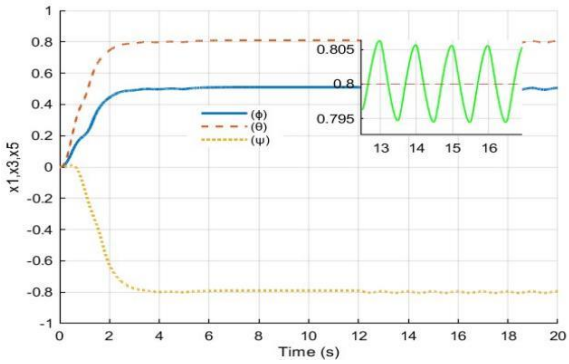

(b) BFASMC

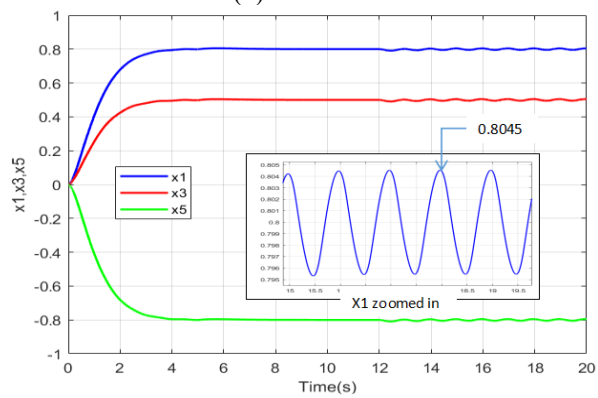

(c) BFISMC

Figure 6. States response

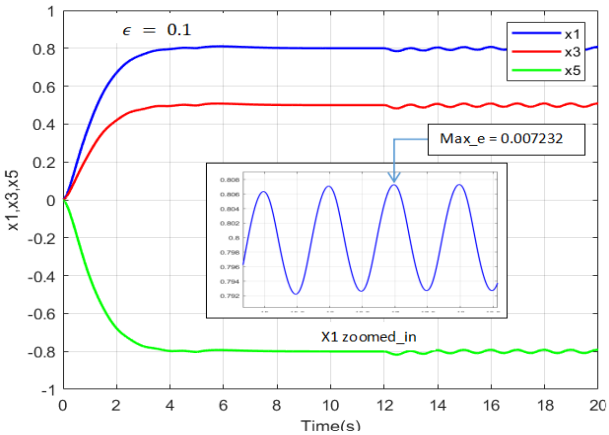

(a) States response with $\epsilon = 0.1$

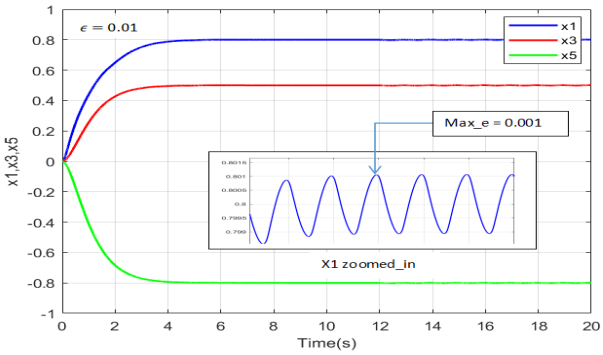

(b) States response with $\epsilon = 0.01$

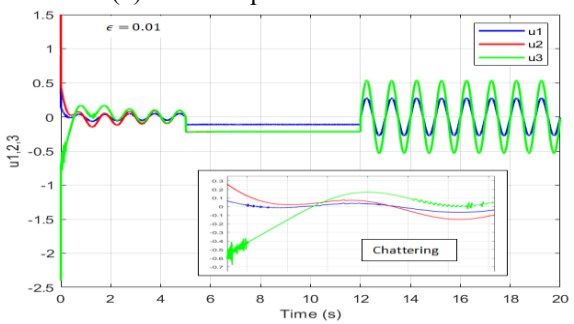

(c) Control inputs with $\epsilon = 0.01$

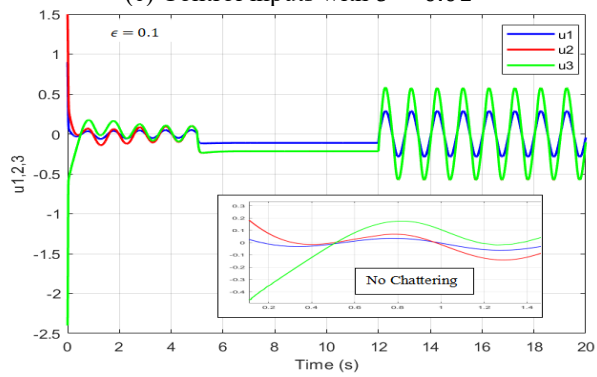

(d) Control inputs with $\epsilon = 0.1$

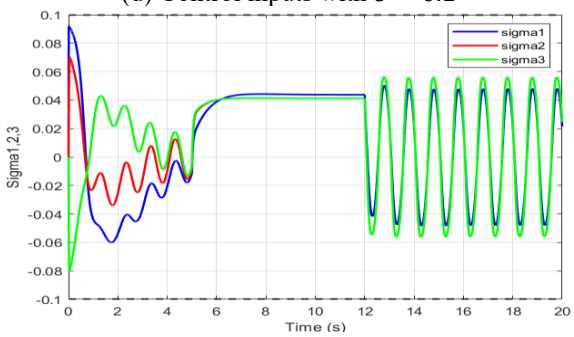

(e) Sliding variable with $\epsilon = 0.1$

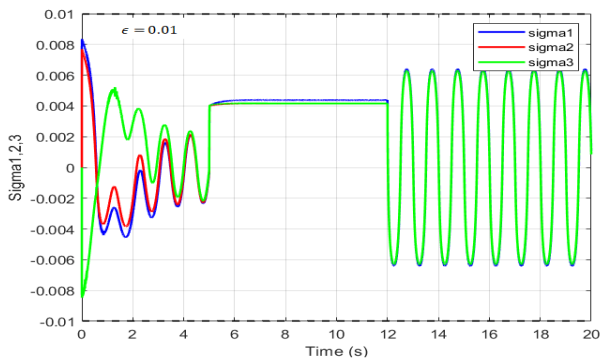

(f) Sliding variable with $\epsilon = 0.01$

Figure 7. States response, sliding variable and control inputs, with $\epsilon = 0.1$ and 0.01

It has been stated that the accuracy of the system's response is inversely proportional to the thickness of the boundary layers, therefore, the choice of Epsilon value is very crucial. To demonstrate this importance, several Epsilon values were used (0.1, 0.05 which has already been used, and 0.01), as shown in Figure 7.

Figure 7 illustrates the effect of the boundary layer width on performance metrics. It can be observed that the upper value of the error in Figure 7(a) is significantly larger compared to the error in Figure 7(b), indicating less accuracy. This is due to the boundary layer width used in both figures which is 0.1 and 0.01 respectively as shown in Table 4.

However, this can lead to real chattering problems in control input, as shown in Figure 7(c) while when using epsilon 0.1 the control is smooth with no chattering as represented in Figure 7(d). Figures 7(e) and (f) introduces the sliding variables within the boundary layer with maximum value of sigma 0.09 and 0.008 respectively. Therefore, careful attention must be paid to selecting the epsilon value tomake a balance between accuracy and the probability ofchattering.

Table 4. Metrics VS ϵ (Channel 1)

Metrics \ ϵ	0.1	0.05	0.01
SSE	0.004616	0.0027	0.00067
Max_E	0.007323	0.004539	0.00106
Chattering	No	No	Yes

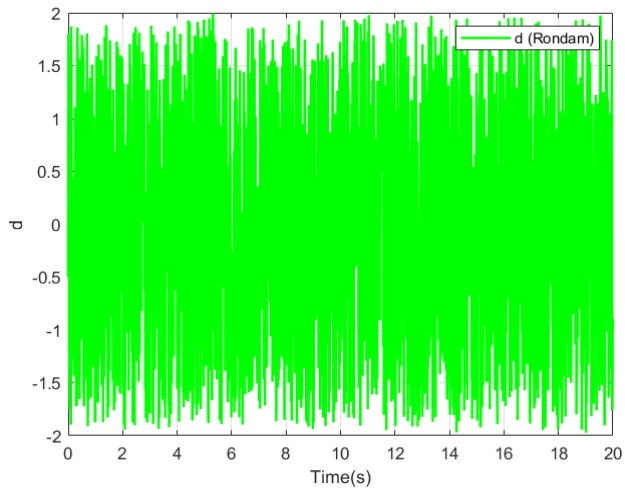

Figure 8. Bounded random disturbance

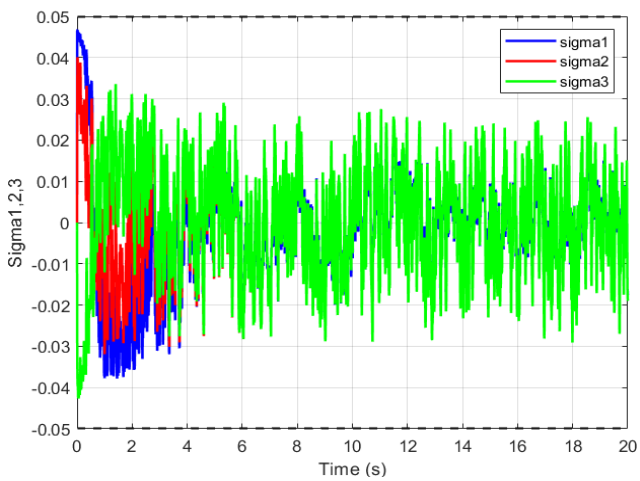

(a) Sliding variables within the boundary layer

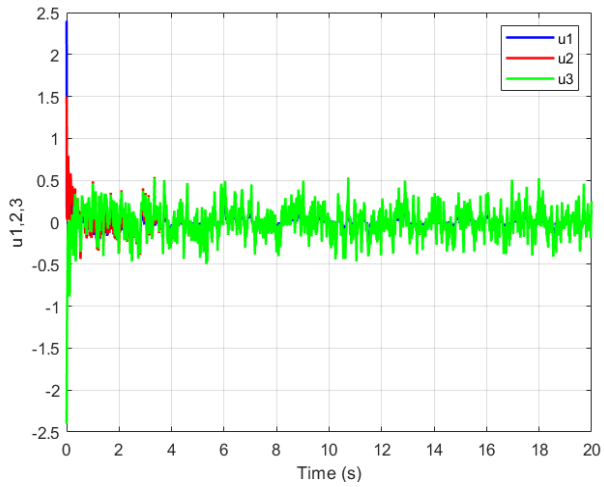

(b) Control inputs

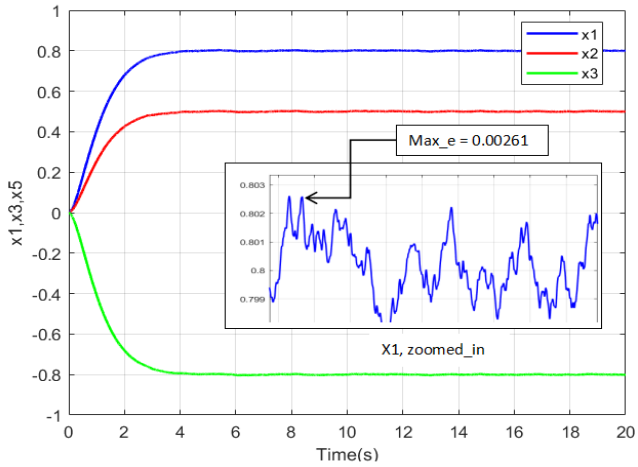

(c) States response

Figure 9. Sliding variables, control inputs and states response with bounded random disturbance

On the other hand, to highlight the validity of the hypothetical controller to counter unexpected disturbance and not requiring prior knowledge of the disturbance dynamics, a bounded random disturbance with ultimate bound = 2 was applied, as shown in Figure 8. Figure 9(a) represents the sliding variables within the predefined boundary layer, while Figure 9(b) introduces the control inputs which follow is the profile of the disturbance to overcome it with the least possible effort to guide the states to their required values with the highest possible accuracy, as presented in Figure 9(c).

Despite the good features of the proposed BFISMC method, its real-world implementation needs improvement, such as the mathematical representation of the complete nonlinear system, consideration of MOI uncertainty due to mass variation, good representation of constraints for actuators bandwidth, saturation, and execution fault.

5. CONCLUSION

This paper presents robust BF based Integral Sliding Mode Control (BFISMC) strategy for Attitude controlling of rigid spacecraft, the proposed method has no reaching phase because of the use of the ISMC, which is known for this property, and no need for prior knowledge of disturbance limits, making it more practical and effective in real-world applications. This method ensures robustness and eliminates chattering under varying conditions by using BF to regulate the gain smoothly. Moreover, this approach is effective in reducing the effect of disturbance, which makes the control system able to behave as nominal full order system from the beginning. In addition, the stability has been proven by Lyapunov criteria, which provides strong theoretical guarantees for the effectiveness of this method. A comparative simulation has been performed, explained that BFISMC outperforms ISMC and BFASMC in terms of adaptability, smoothness and control effort, whereas robust stability and performance were achieved with a steady state error of 0.0026 (rad) and control effort of 0.33 (nm).

REFERENCES

[1] Al-Samarraie, S.A., Salih, M.M. (2017). Adaptive sliding mode controller for servo actuator system with friction. Journal of Engineering, 23(1): 78-95. https://doi.org/10.31026/j.eng.2017.01.06

[2] Li, Z., Chen, X. (2021). Adaptive actuator fault compensation and disturbance rejection scheme for spacecraft. International Journal of Control, Automation and Systems, 19(2): 900-909. https://doi.org/10.1007/s12555-019-0621-4

[3] Gui, H., Vukovich, G. (2017). Adaptive fault-tolerant spacecraft attitude control using a novel integral terminal sliding mode. International Journal of Robust and Nonlinear Control, 27(16): 3174-3196. https://doi.org/10.1002/rnc.3733

[4] Alatorre, A., Espinoza, E.S., Sánchez, B., Ordaz, P., Muñoz, F., Garcia Carrillo, L.R. (2021). Parameter estimation and control of an unmanned aircraft-based transportation system for variable-mass payloads. Asian Journal of Control, 23(5): 2112-2128. https://doi.org/10.1002/asjc.2565

[5] Ordaz, P., Ordaz, M., Cuvas, C., Santos, O. (2019). Reduction of matched and unmatched uncertainties for a class of nonlinear perturbed systems via robust control. International Journal of Robust and Nonlinear Control, 29(8): 2510-2524. https://doi.org/10.1002/rnc.4506

[6] Mohammad, A.M., AL-Samarraie, S.A. (2020). Robust controller design for flexible joint based on back-stepping approach. Iraqi Journal of Computers, Communications, Control and Systems Engineering, 20(2): 58-73. https://doi.org/10.33103/uot.ijccce.20.2.7

[7] Jiang, T., Zhang, F., Lin, D. (2020). Finite-time backstepping for attitude tracking with disturbances and input constraints. International Journal of Control, Automation and Systems, 18(6): 1487-1497. https://doi.org/10.1007/s12555-019-0303-2

[8] Wei, Y., Sheng, D., Chen, Y., Wang, Y. (2019). Fractional order chattering-free robust adaptive backstepping control technique. Nonlinear Dynamics, 95(3): 2383-2394. https://doi.org/10.1007/s11071-018-4698-8

[9] Ji, W., Qiu, J., Karimi, H.R., Fu, Y. (2020). New results on fuzzy integral sliding mode control of nonlinear singularly perturbed systems. IEEE Transactions on Fuzzy Systems, 29(7): 2062-2067. https://doi.org/10.1109/TFUZZ.2020.2985927

[10] Ji, W., Qiu, J., Wu, L., Lam, H.K. (2019). Fuzzy-affine-model-based output feedback dynamic sliding mode controller design of nonlinear systems. IEEE

Transactions on Systems, Man, and Cybernetics: Systems, 51(3): 1652-1661. https://doi.org/10.1109/TSMC.2019.2900050
[11] Vadali, S.R. (1986). Variable-structure control of spacecraft large-angle maneuvers. Journal of Guidance, Control, and Dynamics, 9(2): 235-239. https://doi.org/10.2514/3.20095
[12] Benenia, M., Benslama, M. (2018). Attitude control of a satellite using sliding mode, In 2017 International Conference on Engineering & MIS (ICEMIS), Monastir, Tunisia, pp. 1-4. https://doi.org/10.1109/ICEMIS.2017.8273046
[13] Wang, Q., Wei, Q. (2014). Sliding mode attitude control for flexible spacecraft. In 2014 International Conference on Mechatronics, Control and Electronic Engineering (MCE-14), pp. 545-549. https://doi.org/10.2991/mce-14.2014.122
[14] Zhu, Z., Xia, Y., Fu, M. (2011). Adaptive sliding mode control for attitude stabilization with actuator saturation. IEEE Transactions on Industrial Electronics, 58(10): 4898-4907. https://doi.org/10.1109/TIE.2011.2107719
[15] Wu, B., Wang, D., Poh, E.K. (2013). Decentralized sliding-mode control for attitude synchronization in spacecraft formation. International Journal of Robust and Nonlinear Control, 23(11): 1183-1197. https://doi.org/10.1002/rnc.2812
[16] Zong, Q., Shao, S. (2016). Decentralized finite-time attitude synchronization for multiple rigid spacecraft via a novel disturbance observer. ISA Transactions, 65: 150-163. https://doi.org/10.1016/j.isatra.2016.08.009
[17] Tabatabaee-Nasab, F.S., Naserifar, N. (2021). Nanopositioning control of an electrostatic MEMS actuator: Adaptive terminal sliding mode control approach. Nonlinear Dynamics, 105(1): 213-225. https://doi.org/10.1007/s11071-021-06637-3
[18] Hou, H., Yu, X., Xu, L., Rsetam, K., Cao, Z. (2019). Finite-time continuous terminal sliding mode control of servo motor systems. IEEE Transactions on Industrial Electronics, 67(7): 5647-5656. https://doi.org/10.1109/TIE.2019.2931517
[19] Shao, S., Zong, Q., Tian, B., Wang, F. (2017). Finite-time sliding mode attitude control for rigid spacecraft without angular velocity measurement. Journal of the Franklin Institute, 354(12): 4656-4674. https://doi.org/10.1016/j.jfranklin.2017.04.020
[20] Gan, C., Lu, P., Liu, X., Yang, D. (2014). Distributed cooperative attitude tracking control for multiple rigid spacecraft using fast terminal sliding mode. In Proceeding of the 11th World Congress on Intelligent Control and Automation, Shenyang, China, pp. 2687-2692. https://doi.org/10.1109/WCICA.2014.7053150
[21] Bayat, F., Javaheri, M. (2020). Two-layer terminal sliding mode attitude control of satellites equipped with reaction wheels. Asian Journal of Control, 22(1): 388-397. https://doi.org/10.1002/asjc.1878
[22] Toloei, A., Asgari, H. (2019). Quaternion-based finite-time sliding mode controller design for attitude tracking of a rigid spacecraft during high-thrust orbital maneuver in the presence of disturbance torques. International Journal of Engineering Transactions C: Aspects, 32(3): 430-437. https://doi.org/10.5829/ije.2019.32.03c.11
[23] Wang, Z., Li, Q., Li, S. (2019). Adaptive integral-type terminal sliding mode fault tolerant control for spacecraft attitude tracking. IEEE Access, 7: 35195-35207. https://doi.org/10.1109/ACCESS.2019.2901966
[24] Shao, K. (2021). Nested adaptive integral terminal sliding mode control for high-order uncertain nonlinear systems. International Journal of Robust and Nonlinear Control, 31(14): 6668-6680. https://doi.org/10.1002/rnc.5631
[25] Gong, W., Li, B., Yang, Y., Ban, H., Xiao, B. (2019). Fixed-time integral-type sliding mode control for the quadrotor UAV attitude stabilization under actuator failures. Aerospace Science and Technology, 95: 105444. https://doi.org/10.1016/j.ast.2019.105444
[26] Obeid, H., Fridman, L.M., Laghrouche, S., Harmouche, M. (2018). Barrier function-based adaptive sliding mode control. Automatica, 93: 540-544. https://doi.org/10.1016/j.automatica.2018.03.078
[27] Incremona, G.P., Cucuzzella, M., Ferrara, A. (2016). Adaptive suboptimal second-order sliding mode control for microgrids. International Journal of Control, 89(9): 1849-1867. https://doi.org/10.1080/00207179.2016.1138241
[28] Negrete-Chávez, D.Y., Moreno, J.A. (2016). Second-order sliding mode output feedback controller with adaptation. International Journal of Adaptive Control and Signal Processing, 30(8-10): 1523-1543. https://doi.org/10.1002/acs.2662
[29] Oliveira, T.R., Cunha, J.P.V., Hsu, L. (2016). Adaptive sliding mode control for disturbances with unknown bounds. In 2016 14th International Workshop on Variable Structure Systems (VSS), Nanjing, China, pp. 59-64. https://doi.org/10.1109/VSS.2016.7506891
[30] Wang, Y., Chen, X., Tomizuka, M. (2014). Adaptive sliding mode spacecraft attitude control. Dynamic Systems and Control Conference, DSCC2014-5979, V002T25A001. https://doi.org/10.1115/DSCC2014-5979
[31] Geng, Y., Li, C., Sun, Y., Ma, J. (2016). Adaptive sliding mode attitude tracking control for flexible spacecraft. In 2016 Sixth International Conference on Instrumentation & Measurement, Computer, Communication and Control (IMCCC), Harbin, China, pp. 400-404. https://doi.org/10.1109/IMCCC.2016.69
[32] Yang, J., Stoll, E. (2019). Adaptive sliding mode control for spacecraft proximity operations based on dual quaternions. Journal of Guidance, Control, and Dynamics, 42(11): 2356-2368. https://doi.org/10.2514/1.G004435
[33] Benmansour, J.E. (2020). Satellite attitude control based adaptive sliding mode method. Algerian Journal of Engineering Research, 4(1): 6-11.
[34] Huo, B., Du, M., Yan, Z. (2023). Adaptive sliding mode attitude tracking control for rigid spacecraft considering the unwinding problem. Mathematics, 11(20): 4372. https://doi.org/10.3390/math11204372
[35] Zhang, J., Biggs, J.D., Sun, Z. (2019). Relative orbit-attitude tracking for spacecraft using adaptive fast terminal sliding mode control. In 5th CEAS Specialist Conference on Guidance, Navigation and Control-EuroGNC, Milano, Italy, pp. 1-11.
[36] Zheng, L., Dong, X., Luo, Q., Zeng, M., Yang, X., Zhou, R. (2019). Robust adaptive sliding mode fault tolerant control for nonlinear system with actuator fault and external disturbance. Mathematical Problems in

Engineering, 2019(1): 6349510. https://doi.org/10.1155/2019/6349510
[37] Dong, X., Dong, R., Wu, A.G. (2020). Adaptive dynamic sliding mode control laws for attitude stabilization of flexible spacecraft. Journal of Physics: Conference Series, 1449(1): 012093. https://doi.org/10.1088/1742-6596/1449/1/012093
[38] Shahna, M.H., Abedi, M. (2021). Design of a finite time passivity based adaptive sliding mode control implementing on a spacecraft attitude dynamic simulator. Control Engineering Practice, 114: 104866. https://doi.org/10.1016/j.conengprac.2021.104866
[39] Kuang, J., Chen, M. (2024). Adaptive sliding mode control for trajectory tracking of quadrotor UAV under input saturation and disturbances. Drones, 8: 614. https://doi.org/10.20944/preprints202409.1088.v1
[40] Li, A., Liu, M., Shi, Y. (2020). Adaptive sliding mode attitude tracking control for flexible spacecraft systems based on the Takagi-Sugeno fuzzy modelling method. Acta Astronautica, 175: 570-581. https://doi.org/10.1016/j.actaastro.2020.05.041
[41] Hang, B., Su, B., Deng, W. (2023). Adaptive sliding mode fault-tolerant attitude control for flexible satellites based on ts fuzzy disturbance modeling. Mathematical Biosciences and Engineering, 20(7): 12700-12717. https://doi.org/10.3934/mbe.2023566
[42] Hassan, M.Y., Ad'Doory, M.Q.F. (2007). Design of adaptive fuzzy-neural pid-like controller for nonlinear mimo systems. Iraqi Journal of Computer, Communication, Control and Systems Engineering, 7(1): 1-10.
[43] Incremona, G.P., Mirkin, L., Colaneri, P. (2021). Integral sliding-mode control with internal model: A separation. IEEE Control Systems Letters, 6: 446-451. https://doi.org/10.1109/LCSYS.2021.3079187
[44] Husain, S.S., MohammadRidha, T. (2022). Design of integral sliding mode control for seismic effect regulation on buildings with unmatched disturbance. Mathematical Modelling of Engineering Problems, 9(4): 1123-1130. https://doi.org/10.18280/mmep.090431
[45] Husain, S.S., Al-Dujaili, A.Q., Jaber, A.A., Humaidi, A.J., Al-Azzawi, R.S. (2024). Design of a robust controller based on barrier function for vehicle steer-by-wire systems. World Electric Vehicle Journal, 15(1): 17. https://doi.org/10.3390/wevj15010017
[46] Sultan, T.A., Issa, A.H., Abood, L.H. (2025). Optimized adaptive cascaded integral slide mode controller for a flexible joint manipulator in the presence of uncertainties and disturbances. International Journal of Intelligent Engineering & Systems, 18(8): 566. https://doi.org/10.22266/ijies2025.0930.35
[47] Wie, B. (2008). Space Vehicle Dynamics and Control. Aiaa. American Institute of Aeronautics and Astronautics. https://doi.org/10.2514/4.860119
[48] Goldstein, H., Poole, C., Safko, J. (2011). Classical Mechanics (3rd ed). Addison Wesley.
[49] Wertz, J. (1978). Spacecraft Attitude Determination and Control. Astrophysics and Space Science Library. https://doi.org/10.1007/978-94-009-9907-7
[50] Utkin, V., Guldner, J., Shi, J. (2009). Sliding Mode Control in Electro-Mechanical Systems. Taylor & Francis Group, LLC, 2009. https://doi.org/10.1201/9781420065619
[51] MohammadRidha, T., Al-Samarraie, S.A. (2023). A barrier function-based integral sliding mode control of heart rate during treadmill exercise. Mathematical Modelling of Engineering Problems, 10(1): 179-188. https://doi.org/10.18280/MMEP.100120
[52] Noor, F., Zeb, K., Ullah, S., Ullah, Z., Khalid, M., Al-Durra, A. (2024). Design and validation of adaptive barrier function sliding mode controller for a novel multisource hybrid energy storage system based electric vehicle. IEEE Access, 12: 145270–145285. https://doi.org/10.1109/ACCESS.2024.3471893
[53] Abd, A.F., Al-Samarraie, S.A. (2021). Integral sliding mode control based on barrier function for servo actuator with friction. Engineering and Technology Journal, 39(2): 248-259. https://doi.org/10.30684/etj.v39i2a.1826

NOMENCLATURE

T	Net external torque, N.M
L	Angular momentum, kg.m^2/s
I	Moment of Inertia, kg.m^2
w	Angular velocity, rad/s
u	Control Input, N.M
u_s	Discontinuous control input, N.M
u_n	Nominal control input, N.M
d	Disturbance, N.M
d_{max}	Maximum disturbance N.M
k	Discontinouos control gain
x	State (angle), rad
x_d	Desired position (angle), rad
e	Error, rad
s	Sliding surface
V	Candidate Lyapunov function
z	Integral term

Greek symbols

α	Gain adaptation rate
β	Nominal system gain
ϕ	Roll angle, rad
θ	Pitch angle, rad
ψ	Yaw angle, rad
ρ	Sliding surface convergence rate
σ	Auxiliary sliding surface
ϵ	Boundary layer thikness